Analysis of the trend to equilibrium of a chemically reacting system

2007 J. Phys. A: Math. Theor. 40 2553

(http://iopscience.iop.org/1751-8121/40/10/020)

IOP PUBLISHING JOURNAL OF PHYSICS A: MATHEMATICAL AND THEORETICAL

J. Phys. A: Math. Theor. **40** (2007) 2553–2571 doi:10.1088/1751-8113/40/10/020

Analysis of the trend to equilibrium of a chemically reacting system

Gilberto M Kremer[1], Miriam Pandolfi Bianchi[2] and Ana Jacinta Soares[3]

[1] Departamento de Física, Universidade Federal do Paraná, Curitiba, Brazil
[2] Dipartimento di Matematica, Politecnico di Torino, Torino, Italy
[3] Departamento de Matemática, Universidade do Minho, Braga, Portugal

E-mail: kremer@fisica.ufpr.br, miriam.pandolfi@polito.it and ajsoares@math.uminho.pt

Received 15 August 2006, in final form 30 January 2007
Published 21 February 2007
Online at stacks.iop.org/JPhysA/40/2553

Abstract

In this present paper, a quaternary gaseous reactive mixture, for which the chemical reaction is close to its final stage and the elastic and reactive frequencies are comparable, is modelled within the Boltzmann equation extended to reacting gases. The main objective is a detailed analysis of the non-equilibrium effects arising in the reactive system $A_1 + A_2 \rightleftharpoons A_3 + A_4$, in a flow regime which is considered not far away from thermal, mechanical and chemical equilibrium. A first-order perturbation solution technique is applied to the macroscopic field equations for the spatially homogeneous gas system, and the trend to equilibrium is studied in detail. Adopting elastic hard-spheres and reactive line-of-centres cross sections and an appropriate choice of the input distribution functions—which allows us to distinguish the two cases where the constituents are either at same or different temperatures—explicit computations of the linearized production terms for mass, momentum and total energy are performed for each gas species. The departures from the equilibrium states of densities, temperatures and diffusion fluxes are characterized by small perturbations of their corresponding equilibrium values. For the hydrogen–chlorine system, the perturbations are plotted as functions of time for both cases where the species are either at the same or different temperatures. Moreover, the trend to equilibrium of the reaction rates is represented for the forward and backward reaction $H_2 + Cl \rightleftharpoons HCl + H$.

PACS numbers: 51.10.+y, 47.70.Fw, 82.40.−g

1. Introduction

The description at various levels of physical processes involving gas phase chemical reactions constitutes the object of great efforts of research works since the middle of the past century, for

which the main literature can be found in the extensive bibliography set up by Kennedy [1]. The investigation of chemically reacting flows is in fact fundamental in order to make deeper the knowledge of significant fields as plasma chemistry, atmosphere physics at high altitudes, ionization processes accompanying the re-entry of hypersonic vehicles, chemical technology and several others.

As focused by Shizgal and Chikhaoui in the very recent paper [2] and references cited therein, most production dealing with the chemical kinetic Boltzmann equation (BE) is devoted to study the influence of non-equilibrium effects on the relevant aspects of reactive systems. A chemical reaction that takes place in a gas induces a perturbation of the local equilibrium disturbing the molecular velocity distribution from its Maxwellian form and the reaction rate from its equilibrium value, whereas elastic collisions contribute to restore the equilibrium. These deviations appear to be more relevant at higher atmosphere altitudes where the elastic collisions are not sufficient to sustain the equilibrium of the gas flow [3]. A departure from the Maxwellian velocity distribution, due to the proceeding of the reaction itself, is in general responsible for the reaction rate decrease and may cause qualitative changes of the system properties.

In particular, non-equilibrium effects arising in a dilute gas system whose constituents undergo a bimolecular chemical reaction, were recognized in the pioneering study by Prigogine and collaborators [4, 5] since 1949, for the simple reaction $A + A \rightarrow B + C$. They first generalized the Chapman–Enskog solution [6] of the BE to the case of reacting gases with slow chemical reactions, and showed that the rate coefficient decreases from early stages of the reaction for which the role of products can be neglected.

Many authors then focused on the non-equilibrium velocity distribution functions, searching a perturbation solution of the chemical kinetic BE, under the requirement that the elastic characteristic time—necessary to restore the equilibrium—is shorter than the reactive one, that is the reaction rate is relatively small and the chemical process can be treated as a weak perturbation of the system [7–12]. The extent of the departure of the velocity distributions from the Maxwellians is essentially estimated, as in papers [8, 9] and some others later, from solutions of the chemical kinetic BE obtained via Chapman–Enskog procedure and Sonine polynomial approximation to the coefficients of the distribution functions. The hard sphere elastic and line-of-centres reactive cross sections are commonly adopted, but some other appropriate choices, as Maxwell molecule elastic cross sections and power-law reactive cross sections, can be employed as well [2]. However, there exist different approaches to face the same problem, also in the presence of less simple chemical reactions, as those related to the Grad moments method [13, 14], Monte Carlo [11, 15–20], and molecular dynamics simulations [21–23]. In the above-cited papers, the calculations of the non-equilibrium effects have been performed adopting, at least, one of the following simplified assumptions: the products of the reaction are not taken into account; the effects of the reverse reaction are neglected; one of the constituents, say A, is chosen in large excess, so that collisions among A molecules are neglected; all constituents have a common temperature which is equal to the mixture temperature; the reaction is of type $A + A \rightleftharpoons B + B$, with or without the reverse reaction, so that the masses of the two species are equal. Non-equilibrium effects induced by bimolecular reversible [24–27] and irreversible [28] reactions have been investigated by means of various approaches based on the Chapman–Enskog method also in view of transport properties. Owing to the reactive process, the temperatures of the constituents recover a meaningful role in chemically reactive flows [9, 29–32]. This circumstance affects the departure of the reaction rate coefficients from their equilibrium value, as widely discussed in the literature [2, 11, 16].

The main purpose of this present paper is to characterize the non-equilibrium effects on macroscopic fields induced by a bimolecular reaction of type $A_1 + A_2 \rightleftharpoons A_3 + A_4$, in a more

general case than in the above-cited papers, in the absence of the said simplified assumptions. The gaseous chemical system of four constituents is examined near the chemical equilibrium when the elastic and reactive characteristic frequencies are comparable, and the chemical reaction is considered a fast process. Calculations are performed for a model of reactive hard spheres. Two cases are analysed with reference to the assumption of constituents either at same or different temperatures. The inclusion of the reverse reaction induces perturbations on the reaction rate which depends on other system parameters related to the backward reaction. Moreover, in the case of constituents at different temperatures, the reaction rate exhibits an explicit dependence on the individual temperatures. A mathematical procedure, based on a first-order perturbation expansion of the system variables around the thermal, mechanical and chemical equilibrium, is applied to the balance field equations. An explicit computation of the elastic and reactive production terms which figure in the balance equations is performed under the above-specified temperature assumptions. In the first case, the input velocity distributions for the constituents are expressed in terms of Maxwellians at the same temperature, plus a small non-equilibrium term which depends on the diffusion velocities. In the second case, the correction that arises owing to the reactive process, exhibits a further linear dependence on the different species temperatures. The flow regime of interest here is that for which the chemical reaction is very fast, that is the reaction time is much smaller than the flow time. Therefore, the Damkohler number [34], which is a measure of the ratio of the scale on which reaction takes place, assumes rather large values. The effects due to a lower range of Damkohler number can be exploited when the model is referred to the continuum limit at the Navier–Stokes level.

The macroscopic field equations are written for the spatially homogeneous gas as a set of coupled linearized ordinary differential equations, assuming that the macroscopic variables are time-dependent only. The role of the temperature in the two mentioned cases is emphasized with regard to the flow behaviour towards equilibrium. A detailed analysis of the perturbations related to species temperatures, concentrations, diffusion fluxes, forward and backward reaction rates, as well as affinity, is performed for the hydrogen–chlorine system.

The paper is organized as follows. In section 2 some preliminaries are recalled concerning the mathematical formulation of the chemical kinetic BE for the quaternary gas mixture. The corresponding macroscopic field equations, namely the balance equations and the conservation laws, are deduced in the absence of external fields. In section 3, the linearized production terms for mass, momentum and total energy are computed explicitly. The hard-sphere model for the elastic collisions and the 'line of centres' model [33] for the reactive collisions are assumed, and the input distributions are considered as local Maxwellians with species temperatures, expanded in the mixture rest frame. In section 4, the system of linearized field equations for the macroscopic variables are obtained for the two considered cases. The asymptotic behaviours of the perturbations with respect to time are analysed in section 5 for the reaction $H_2 + Cl \rightleftharpoons HCl + H$ by imposing different initial conditions.

2. The reactive system

Consider a gaseous mixture of four constituents A_α with molecular mass m_α and formation energy ε_α, undergoing a reversible bimolecular reaction of type

$$A_1 + A_2 \rightleftharpoons A_3 + A_4. \tag{1}$$

Masses, momenta and energies are arranged so that the conservation laws hold

$$m_1 + m_2 = m_3 + m_4, \qquad m_1\mathbf{c}_1 + m_2\mathbf{c}_2 = m_3\mathbf{c}_3 + m_4\mathbf{c}_4, \tag{2}$$

$$\varepsilon_1 + \tfrac{1}{2}m_1c_1^2 + \varepsilon_2 + \tfrac{1}{2}m_2c_2^2 = \varepsilon_3 + \tfrac{1}{2}m_3c_3^2 + \varepsilon_4 + \tfrac{1}{2}m_4c_4^2, \tag{3}$$

where ε_α represent the formation energy of constituent α whereas $(\mathbf{c}_1, \mathbf{c}_2)$ and $(\mathbf{c}_3, \mathbf{c}_4)$ are the velocities of reactants and products, for the forward reaction, respectively. The gas is characterized in the phase space by the set of one-particle distribution functions $f_\alpha \equiv f(\boldsymbol{x}, \boldsymbol{c}_\alpha, t), \alpha = 1, \ldots, 4$, with $f_\alpha \, \mathrm{d}\boldsymbol{x} \, \mathrm{d}\boldsymbol{c}_\alpha$ denoting the number of α-particles in the volume element $\mathrm{d}\boldsymbol{x} \, \mathrm{d}\boldsymbol{c}_\alpha$ around position $\boldsymbol{x}$ and velocity $\boldsymbol{c}_\alpha$, at time t.

2.1. Reactive kinetic equations

In the absence of external body forces, the distribution functions f_α satisfy the following chemical kinetic Boltzmann equation

$$\frac{\partial f_\alpha}{\partial t} + c_i^\alpha \frac{\partial f_\alpha}{\partial x_i} = \sum_{\beta=1}^{4} \mathcal{Q}_{\alpha\beta}^E + \mathcal{Q}_\alpha^R, \tag{4}$$

where the collision operator, according to the formalism of paper [25], splits into the contributions $\mathcal{Q}_{\alpha\beta}^E$ for elastic scattering and $\mathcal{Q}_{\alpha\gamma}^R$ for interactions with chemical reaction, which read

$$\mathcal{Q}_{\alpha\beta}^E = \int (f'_\alpha f'_\beta - f_\alpha f_\beta) g_{\beta\alpha} \sigma_{\beta\alpha} \, \mathrm{d}\Omega_{\beta\alpha} \, \mathrm{d}\mathbf{c}_\beta, \tag{5}$$

$$\mathcal{Q}_{1(2)}^R = \int \left[f_3 f_4 \left(\frac{m_1 m_2}{m_3 m_4} \right)^3 - f_1 f_2 \right] \sigma_{12}^\star g_{21} \, \mathrm{d}\Omega \, \mathrm{d}\mathbf{c}_{2(1)}, \tag{6}$$

$$\mathcal{Q}_{3(4)}^R = \int \left[f_1 f_2 \left(\frac{m_3 m_4}{m_1 m_2} \right)^3 - f_3 f_4 \right] \sigma_{34}^\star g_{43} \, \mathrm{d}\Omega' \, \mathrm{d}\mathbf{c}_{4(3)}. \tag{7}$$

In the above equations $g_{\beta\alpha} = |\boldsymbol{c}_\beta - \boldsymbol{c}_\alpha|$ is a relative velocity, $\mathrm{d}\Omega_{\alpha\beta}$ and $\mathrm{d}\Omega$ are elements of solid angles which characterize the scattering processes, $\sigma_{\alpha\beta}$ is the differential elastic cross section, $\sigma_{12}^\star$ and $\sigma_{34}^\star$ are differential reactive cross sections for forward and backward reaction, respectively, related by the micro-reversibility principle in the form

$$\sigma_{34}^\star = \left(\frac{m_1 m_2}{m_3 m_4} \right)^2 \left(\frac{g_{21}}{g_{43}} \right)^2 \sigma_{12}^\star. \tag{8}$$

The chemical kinetics of the system, neglecting the internal degrees of freedom for the gas molecules such as rotational and vibrational energies, is based on the following form of the chemical potential of each constituent

$$\mu_\alpha = \varepsilon_\alpha - kT \left[\frac{3}{2} \ln T - \ln n_\alpha + \frac{3}{2} \ln \left(\frac{2\pi m_\alpha k}{h^2} \right) \right], \tag{9}$$

where n_α denotes the particle number density of each constituent, k is the Boltzmann constant, h is the Planck constant and T is the temperature of the mixture.

For the reversible reaction (1), the affinity, which characterizes the deviation of the system from the chemical equilibrium, is defined [35] by

$$\mathcal{A} = -\sum_{\alpha=1}^{4} \nu_\alpha \mu_\alpha, \tag{10}$$

where the stoichiometric coefficients are such that $\nu_1 = \nu_2 = -\nu_3 = -\nu_4 = -1$ and the chemical equilibrium condition assumes the form

$$\mu_1^{\mathrm{eq}} + \mu_2^{\mathrm{eq}} = \mu_3^{\mathrm{eq}} + \mu_4^{\mathrm{eq}}. \tag{11}$$

The mass action law is obtained from equations (9) and (11) as

$$E^\star \equiv \frac{E}{kT} = \frac{3}{2}\ln\left(\frac{m_3 m_4}{m_1 m_2}\right) + \ln\left(\frac{n_1^{\mathrm{eq}} n_2^{\mathrm{eq}}}{n_3^{\mathrm{eq}} n_4^{\mathrm{eq}}}\right), \tag{12}$$

where $E = \varepsilon_3 + \varepsilon_4 - \varepsilon_1 - \varepsilon_2$ is the binding energy difference between products and reagents, and $E^\star$ is given in units of the thermal energy of the mixture, kT. Thus the detailed expression for the affinity follows from equations (9), (10) and (12) in the form

$$\mathcal{A} = kT\ln\left(\frac{n_1 n_2 n_3^{\mathrm{eq}} n_4^{\mathrm{eq}}}{n_3 n_4 n_1^{\mathrm{eq}} n_2^{\mathrm{eq}}}\right), \tag{13}$$

with $\mathcal{A} = 0$ in chemical equilibrium conditions. In the above equations, the upper index 'eq' denotes equilibrium values.

2.2. Balance equations and conservation laws

The balance equations for mass, momentum and energy density of each constituent give the macroscopic description of the reacting system and are classically derived from the BE (4) in the form [26]

$$\frac{\partial \varrho_\alpha}{\partial t} + \frac{\partial}{\partial x_i}\left(\varrho_\alpha u_i^\alpha + \varrho_\alpha v_i\right) = \int m_\alpha \left(\sum_{\beta=1}^{4} \mathcal{Q}_{\alpha\beta}^E + \mathcal{Q}_\alpha^R\right) \mathrm{d}\mathbf{c}_\alpha, \tag{14}$$

$$\frac{\partial \varrho_\alpha v_i^\alpha}{\partial t} + \frac{\partial}{\partial x_j}\left(p_{ij}^\alpha + \varrho_\alpha u_i^\alpha v_j + \varrho_\alpha u_j^\alpha v_i + \varrho_\alpha v_i v_j\right) = \int m_\alpha c_i^\alpha \left(\sum_{\beta=1}^{4} \mathcal{Q}_{\alpha\beta}^E + \mathcal{Q}_\alpha^R\right) \mathrm{d}\mathbf{c}_\alpha, \tag{15}$$

$$\begin{aligned}\frac{\partial}{\partial t}\left[\frac{3}{2}p_\alpha + n_\alpha\varepsilon_\alpha + \varrho_\alpha u_i^\alpha v_i + \frac{1}{2}\varrho_\alpha v^2\right] + \frac{\partial}{\partial x_i}\Bigg[q_i^\alpha + p_{ij}^\alpha v_j + n_\alpha\varepsilon_\alpha u_i^\alpha + \frac{1}{2}\varrho_\alpha u_i^\alpha v^2 \\ + \left(\frac{3}{2}p_\alpha + n_\alpha\varepsilon_\alpha + \varrho_\alpha u_j^\alpha v_j + \frac{1}{2}\varrho_\alpha v^2\right) v_i\Bigg] \\ = \int \left(\frac{1}{2}m_\alpha c_\alpha^2 + \varepsilon_\alpha\right)\left(\sum_{\beta=1}^{4} \mathcal{Q}_{\alpha\beta}^E + \mathcal{Q}_\alpha^R\right) \mathrm{d}\mathbf{c}_\alpha.\end{aligned} \tag{16}$$

The macroscopic observables are defined in terms of the distribution function for each constituent α by

$$\varrho_\alpha = \int m_\alpha f_\alpha \,\mathrm{d}\mathbf{c}_\alpha = m_\alpha n_\alpha, \qquad \text{with} \quad \varrho = \sum_{\alpha=1}^{4}\varrho_\alpha \qquad \text{and} \qquad n = \sum_{\alpha=1}^{4} n_\alpha, \tag{17}$$

$$\varrho_\alpha v_i^\alpha = \int m_\alpha c_i^\alpha f_\alpha \,\mathrm{d}\mathbf{c}_\alpha, \qquad \text{with} \quad \varrho v_i = \sum_{\alpha=1}^{4}\varrho_\alpha v_i^\alpha, \tag{18}$$

$$u_i^\alpha = \frac{1}{\varrho_\alpha}\int m_\alpha \xi_i^\alpha f_\alpha \,\mathrm{d}\mathbf{c}_\alpha, \qquad \text{with} \quad \xi_i^\alpha = c_i^\alpha - v_i \qquad \text{and} \qquad \sum_{\alpha=1}^{4}\varrho_\alpha u_i^\alpha = 0, \tag{19}$$

$$p_{ij}^\alpha = \int m_\alpha \xi_i^\alpha \xi_j^\alpha f_\alpha \,\mathrm{d}\mathbf{c}_\alpha, \qquad \text{with} \quad p_{ij} = \sum_{\alpha=1}^{4} p_{ij}^\alpha, \tag{20}$$

$$p_\alpha = \frac{1}{3}\int m_\alpha \xi_\alpha^2 f_\alpha \,\mathrm{d}\mathbf{c}_\alpha, \qquad \text{with} \quad p = \sum_{\alpha=1}^{4} p_\alpha, \tag{21}$$

$$T_\alpha = \frac{p_\alpha}{n_\alpha k}, \qquad \text{with} \quad T = \sum_{\alpha=1}^{4} \frac{n_\alpha}{n} T_\alpha = \frac{p}{nk}, \tag{22}$$

$$q_i^\alpha = \int \frac{1}{2} m_\alpha \xi_\alpha^2 \xi_i^\alpha f_\alpha \,\mathrm{d}\mathbf{c}_\alpha, \qquad \text{with} \quad q_i = \sum_{\alpha=1}^{4} \left(q_i^\alpha + n_\alpha \varepsilon_\alpha u_i^\alpha\right). \tag{23}$$

Above ϱ_α, p_α, T_α, v_i^α, ξ_i^α, u_i^α, p_{ij}^α and q_i^α denote the mass density, pressure, temperature and the components of the velocity, peculiar velocity, diffusion velocity, pressure tensor and heat flux for each constituent α, respectively. Moreover, ϱ, n, p, T, p_{ij} and q_i represent the mass density, particle number density, pressure, temperature and components of the pressure tensor and heat flux of the whole mixture, respectively. Note that due to the constraint $(19)_3$ there exist only three independent diffusion velocities. Furthermore, the term $n_\alpha \varepsilon_\alpha u_i^\alpha$ which figures in the expression of q_i refers to the formation energy transfer of a molecule of constituent α due to diffusion.

Since mass, momentum and total energy are preserved during both elastic and reactive collisions, the following conditions hold true:

$$\sum_{\alpha=1}^{4}\sum_{\beta=1}^{4}\int \psi_\alpha \mathcal{Q}_{\alpha\beta}^E \,\mathrm{d}\mathbf{c}_\alpha = 0, \qquad \sum_{\alpha=1}^{4}\int \psi_\alpha \mathcal{Q}_\alpha^R \,\mathrm{d}\mathbf{c}_\alpha = 0, \tag{24}$$

for the so-called summational invariants $\psi_\alpha = m_\alpha, \psi_\alpha = m_\alpha c_i^\alpha$ and $\psi_\alpha = \frac{1}{2} m_\alpha c_\alpha^2 + \varepsilon_\alpha$, alternatively. The conservation equations for mass, momentum and temperature of the whole mixture are then obtained by summing equations (14)–(16) over all constituents, in the form

$$\frac{\partial \varrho}{\partial t} + \frac{\partial}{\partial x_i}(\varrho v_i) = 0, \tag{25}$$

$$\frac{\partial \varrho v_i}{\partial t} + \frac{\partial}{\partial x_j}(p_{ij} + \varrho v_i v_j) = 0, \tag{26}$$

$$\frac{\partial}{\partial t}\left[\frac{3}{2}nkT + \sum_{\alpha=1}^{4} n_\alpha \varepsilon_\alpha + \frac{1}{2}\varrho v^2\right] + \frac{\partial}{\partial x_i}\left[q_i + p_{ij} v_j + \left(\frac{3}{2}nkT + \sum_{\alpha=1}^{4} n_\alpha \varepsilon_\alpha + \frac{1}{2}\varrho v^2\right) v_i\right] = 0. \tag{27}$$

3. Linearized elastic and reactive production terms

In order to deduce the explicit expressions for the elastic and reactive production terms which appear in the balance equations of mass (14), momentum (15) and total energy (16), differential elastic cross sections of rigid spheres are assumed for which

$$\sigma_{\alpha\beta} = \tfrac{1}{4} d_{\alpha\beta}^2, \qquad d_{\alpha\beta} = \tfrac{1}{2}(d_\alpha + d_\beta), \tag{28}$$

where d_α and d_β are the diameters of the colliding spheres. The reactive cross sections, according to the line-of-centres model [33], are those for which the kinetic energy of colliding spheres exceeds the activation energy, namely

$$\sigma_{\alpha\beta}^\star = \begin{cases} 0, & \gamma_{\alpha\beta} \leqslant \epsilon_\sigma^\star \\ \dfrac{1}{4} d_\sigma^2 \left(1 - \dfrac{\epsilon_\sigma^\star}{\gamma_{\alpha\beta}}\right), & \gamma_{\alpha\beta} > \epsilon_\sigma^\star. \end{cases} \tag{29}$$

In definition (29), d_σ represents a reactive collision diameter, $\gamma_{\alpha\beta} = m_{\alpha\beta} g_{\beta\alpha}^2 / 2kT$ is the relative translational energy, $\epsilon_\sigma^\star = \epsilon_\sigma / kT$ is the activation energy in units of kT, and the index σ assumes either the value +1 for the reactants ($\alpha = 1, 2$), or -1 for the products ($\alpha = 3, 4$) of the reaction. Thus, $\epsilon_1^\star$ denotes the forward activation energy, whereas $\epsilon_{-1}^\star = \epsilon_1^\star - E^\star$ the backward activation energy. The elastic and reactive diameters are connected by the steric factor s_σ, namely

$$d_\sigma = s_\sigma d_{\alpha\beta}, \qquad \text{with} \quad s_{-1} = \sqrt{\frac{m_{12}}{m_{34}}} \frac{d_{12}}{d_{34}} s_1 \qquad \text{and} \qquad 0 \leqslant s_1 \leqslant 1, \tag{30}$$

where $m_{12} = m_1 m_2/(m_1 + m_2)$, $m_{34} = m_3 m_4/(m_3 + m_4)$ are reduced masses.

The assumption of differential cross sections given by equations (28) and (29), together with an appropriate choice of input distribution function, allows us to perform all the integrations which are necessary to compute the production terms. At this end, the needed distribution is assumed as an approximation of a local Maxwellian in the constituent rest frame with temperature T_α and velocity v_i^α:

$$f_\alpha = n_\alpha \left(\frac{m_\alpha}{2\pi k T_\alpha} \right)^{\frac{3}{2}} \mathrm{e}^{-\frac{m_\alpha (c_i^\alpha - v_i^\alpha)^2}{2kT_\alpha}}. \tag{31}$$

The velocity distribution (31) is then approximated, through an expansion at the first order, around a Maxwellian in the mixture rest frame with temperature T, by the expansion

$$f_\alpha = n_\alpha \left(\frac{m_\alpha}{2\pi k T} \right)^{\frac{3}{2}} \mathrm{e}^{-\frac{m_\alpha \xi_\alpha^2}{2kT}} \left[1 + \frac{m_\alpha \xi_i^\alpha}{kT} u_i^\alpha + \left(\frac{m_\alpha \xi_\alpha^2}{2kT} - \frac{3}{2} \right) \Delta_\alpha \right], \tag{32}$$

where $\Delta_\alpha = (T_\alpha - T)/T$ and $u_i^\alpha = v_i^\alpha - v_i$. The input function (32) thus represents a linearization of the Maxwellian distribution (31), with respect to the diffusion velocity u_i^α and temperature difference Δ_α. It is relevant to observe that the individual particle number densities n_α are not correlated by the chemical equilibrium condition (11). For this reason, the input function (32) can be regarded as a deviation from the mechanical equilibrium only. The dependence of the input function (32) on each species temperature allows one to appreciate the mixture effects in a more detailed fashion than in the previous works [11, 29, 32] for what concerns the reaction mechanism and heat exchanges.

The computation of the linearized elastic production terms, for $\alpha, \beta = 1, \ldots, 4$, then leads to the following expressions:

$$\int m_\alpha \mathcal{Q}_{\alpha\beta}^E \, \mathrm{d}\mathbf{c}_\alpha = 0, \tag{33}$$

$$\int m_\alpha c_i^\alpha \mathcal{Q}_{\alpha\beta}^E \, \mathrm{d}\mathbf{c}_\alpha = -\frac{8}{3} d_{\alpha\beta}^2 \sqrt{\frac{2\pi kT}{m_{\alpha\beta}}} n_\alpha n_\beta m_{\alpha\beta} \left(u_i^\alpha - u_i^\beta \right), \tag{34}$$

$$\int \left(\frac{1}{2} m_\alpha c_\alpha^2 + \varepsilon_\alpha \right) \mathcal{Q}_{\alpha\beta}^E \, \mathrm{d}\mathbf{c}_\alpha = v_i \int m_\alpha \xi_i^\alpha \mathcal{Q}_{\alpha\beta}^E \, \mathrm{d}\mathbf{c}_\alpha + 8 \sqrt{\frac{2\pi kT}{m_{\alpha\beta}}} n_\alpha n_\beta kT d_{\alpha\beta}^2 M_\alpha M_\beta (\Delta_\beta - \Delta_\alpha). \tag{35}$$

The computation of the linearized reactive production terms proceeds in an analogous way, leading to

$$\int m_\alpha \mathcal{Q}_\alpha^R \mathrm{d}\mathbf{c}_\alpha = \nu_\alpha m_\alpha n_\alpha^{\mathrm{eq}} n_\gamma^{\mathrm{eq}} k_\sigma^{(0)} \times \left\{ \frac{\mathcal{A}}{kT} - \sum_{\beta=1}^{4} \nu_\beta (1 - M_\beta) \left[\left(\epsilon_\sigma^* + \frac{1}{2} \right) - \sigma E^* (1 - \delta_{\alpha\beta} - \delta_{\gamma\beta}) \right] \Delta_\beta \right\}, \tag{36}$$

$$\int m_\alpha c_i^\alpha \mathcal{Q}_\alpha^R \,\mathrm{d}\mathbf{c}_\alpha = v_i \int m_\alpha \mathcal{Q}_\alpha^R \,\mathrm{d}\mathbf{c}_\alpha + m_\alpha n_\alpha^{\mathrm{eq}} n_\gamma^{\mathrm{eq}} k_\sigma^{(0)} \times \left[\sigma \sum_{\beta=1}^{4} \nu_\beta M_\beta u_i^\beta - \frac{2}{3}(\epsilon_\sigma^\star + 2) M_\gamma \left(u_i^\alpha - u_i^\gamma \right) \right], \tag{37}$$

$$\begin{aligned}\int \left(\frac{1}{2} m_\alpha c_\alpha^2 + \varepsilon_\alpha \right) \mathcal{Q}_\alpha^R \,\mathrm{d}\mathbf{c}_\alpha &= \left(\frac{1}{2} m_\alpha v^2 + \varepsilon_\alpha \right) \int \mathcal{Q}_\alpha^R \,\mathrm{d}\mathbf{c}_\alpha + v_i \int m_\alpha \xi_i^\alpha \mathcal{Q}_\alpha^R \,\mathrm{d}\mathbf{c}_\alpha \\ &+ \frac{1}{2} kT n_\alpha^{\mathrm{eq}} n_\gamma^{\mathrm{eq}} k_\sigma^{(0)} \Bigg\{ \nu_\alpha [3M_\alpha + 2M_\gamma (\epsilon_\sigma^\star + 2)] \frac{\mathcal{A}}{kT} \\ &+ M_\alpha \sigma \sum_{\beta=1}^{4} \nu_\beta \Bigg[\frac{15}{2} M_\beta - \frac{9}{2} + 3(\epsilon_\sigma^\star + 2)(1 - M_\beta) \left(1 - \frac{m_\gamma}{m_\alpha} \right) \\ &+ 4(1 - M_\alpha)(\delta_{\alpha\beta} - \delta_{\gamma\beta})(\epsilon_\sigma^\star + 2) - 3\sigma E^\star (1 - M_\beta)(1 - \delta_{\alpha\beta} - \delta_{\gamma\beta}) \\ &+ 2 \frac{m_\gamma}{m_\alpha} (1 - M_\beta) \left[\epsilon_\sigma^{\star\,2} + 4\epsilon_\sigma^\star + 6 - \sigma (1 - \delta_{\alpha\beta} - \delta_{\gamma\beta}) E^\star (\epsilon_\sigma^\star + 2) \right] \Bigg] \Delta_\beta \Bigg\}. \end{aligned} \tag{38}$$

Above, $(\alpha, \gamma) = (1, 2), (2, 1), (3, 4), (4, 3)$ and $M_\alpha = m_\alpha/(m_\alpha + m_\gamma)$. Moreover, $k_\sigma^{(0)}$ denotes the first approximation to the rate constant and assumes the form

$$k_1^{(0)} = \sqrt{\frac{8\pi kT}{m_{12}}}\, \mathrm{e}^{-\epsilon_\mathrm{i}^\star} (s_1 d_{12})^2, \qquad k_{-1}^{(0)} = \frac{n_1^{\mathrm{eq}} n_2^{\mathrm{eq}}}{n_3^{\mathrm{eq}} n_4^{\mathrm{eq}}} k_1^{(0)}, \tag{39}$$

for the forward and backward reactions, respectively.

4. First-order perturbation technique

In this section, spatially homogeneous solutions of the field equations are analysed with the purpose of determining the trend to equilibrium of a mixture of chemically reacting gases. Two cases will be examined separately. In the first case, the constituents are at the same temperature and the reacting system is described by the balance equations (14) and (15) for mass density and diffusion velocity of each constituent α, and the conservation equation (27) for total energy of the whole mixture. Conversely, in the second case, the constituents are assumed at different temperatures and the reacting system is described by equations (14) and (15) as in the first case, but the balance equation (16) for the total energy of each constituent α is considered in place of the conservation equation (27).

4.1. Linearized field equations with constituents at same temperature

The thermodynamical description of a mixture whose constituents are at the same temperature, which is the temperature of the mixture, is determined by the knowledge of the basic fields of partial particle number densities n_α, partial velocities v_i^α and temperature of the mixture T. The field equations for these basic fields are given, as anticipated, by the balance equations (14), (15) and (27). In the spatially homogeneous case, the fields do depend only on time and for processes close to the equilibrium state one can write the partial particle number densities as

$$n_\alpha(t) = n_\alpha^{\mathrm{eq}} [1 + \overline{n}_\alpha(t)], \qquad (\alpha = 1, \ldots, 4) \tag{40}$$

where $\overline{n}_\alpha(t)$ is a small deviation from the equilibrium state. Without loss of generality the x-axis is chosen for the perturbation of the partial velocities, or equivalently for the diffusion velocities, in such a fashion that

$$u_x^\alpha(t) = \overline{u}_\alpha(t), \qquad (\alpha = 1, \ldots, 4) \qquad \text{with} \quad \sum_{\alpha=1}^{4} m_\alpha n^{\text{eq}} x_\alpha^{\text{eq}} \overline{u}_\alpha(t) = 0. \tag{41}$$

The quantity $\overline{u}_\alpha(t)$ is also considered as a small perturbation from equilibrium. Furthermore, the temperature field is written as

$$T(t) = T_{\text{eq}}[1 + \overline{T}(t)], \tag{42}$$

where $\overline{T}(t)$ is a small perturbation of the temperature field from the equilibrium temperature T_{eq}.

From the definition of the affinity (13) and the relationships (40) and (42) one can obtain that the affinity is given by

$$\frac{\mathcal{A}}{kT_{\text{eq}}} = \overline{n}_1(t) + \overline{n}_2(t) - \overline{n}_3(t) - \overline{n}_4(t). \tag{43}$$

The insertion of (33)–(38), by considering $\Delta_\alpha = 0$, together with (40)–(43) into the balance equations (14), (15) and (27) leads to a linearized system of differential equations for $\overline{n}_\alpha, \overline{u}_\alpha$ and $\overline{T}$ which reads

$$x_\alpha^{\text{eq}} \frac{\mathrm{d}\overline{n}_\alpha}{\mathrm{d}t} = \nu_\alpha x_\alpha^{\text{eq}} \zeta_{\alpha\gamma}^R (\overline{n}_1 + \overline{n}_2 - \overline{n}_3 - \overline{n}_4) \equiv \tau_\alpha, \qquad \alpha = 1, \ldots, 4. \tag{44}$$

$$\begin{aligned} \frac{\mathrm{d}\overline{u}_\alpha}{\mathrm{d}t} &= -\sum_{\beta=1}^{4} \zeta_{\alpha\beta}^E M_\beta (\overline{u}_\alpha - \overline{u}_\beta) \\ &\quad + \zeta_{\alpha\gamma}^R \left[\sigma \sum_{\beta=1}^{4} \nu_\beta M_\beta \overline{u}_\beta - \frac{2}{3}(\epsilon_\sigma^\star + 2) M_\gamma (\overline{u}_\alpha - \overline{u}_\gamma) \right], \qquad \alpha = 1, \ldots, 4. \end{aligned} \tag{45}$$

$$\frac{\mathrm{d}\overline{T}}{\mathrm{d}t} = -\frac{2}{3} x_1^{\text{eq}} \zeta_{12}^R E^\star (\overline{n}_1 + \overline{n}_2 - \overline{n}_3 - \overline{n}_4). \tag{46}$$

In the above equations τ_α represents the reaction rate density of constituent α whereas $\zeta_{\alpha\beta}^E$ and $\zeta_{\alpha\gamma}^R$ are elastic and reactive collision frequencies, respectively, defined by

$$\zeta_{\alpha\beta}^E = \frac{8}{3} d_{\alpha\beta}^2 \sqrt{\frac{2\pi kT}{m_{\alpha\beta}}} n_\beta^{\text{eq}}, \qquad \zeta_{\alpha\gamma}^R = n_\gamma^{\text{eq}} k_\sigma^{(0)}. \tag{47}$$

Equations (44) together with (46) represent a coupled system of five linearized differential equations for the partial particle number densities and temperature of the mixture, whereas equations (45) represent a coupled system of three linearized differential equations for the partial diffusion velocities, since due to the constraint $(41)_2$ only three among the four equations (45) are linearly independent.

The system of linearized differential equations (44) and (46) is solved in subsection 5.1 for two sets of initial conditions corresponding to an equilibrium temperature of the mixture and either positive or negative affinity of the reaction. The system (45) is solved in subsection 5.1 as well for initial conditions corresponding first to a diffusion of the reactants with products at rest, and then to a diffusion of the products with reactants at rest.

4.2. Linearized field equations with constituents at different temperatures

For a mixture whose constituents are at different temperatures, the thermodynamical description is determined by the knowledge of the basic fields of partial particle number densities n_α, partial velocities v_i^α and partial temperatures T_α. Now the field equations are obtained from the balance equations (14), (15) and (16) together with (33)–(38). The linearized field equations for the diffusion velocities are the same as those derived in the previous subsection for constituents at same temperature, namely equations (45), thus they will not be analysed here.

The search of spatially homogeneous solutions for the partial particle number densities and temperature employs (40) together with the expansion

$$T_\alpha(t) = T_{\rm eq}[1 + \Delta_\alpha(t)], \qquad (\alpha = 1, \ldots, 4) \tag{48}$$

which represent the temperature deviations of the constituents from the equilibrium temperature of the mixture. Moreover, the deviation of the temperature of the mixture becomes $\overline{T} = \sum_{\alpha=1}^{4} x_\alpha^{\rm eq} \Delta_\alpha$, thanks to Dalton's law [36].

The system of linearized differential equations for the partial particle number densities and temperatures reads

$$\frac{{\rm d}\overline{n}_\alpha}{{\rm d}t} = \nu_\alpha \zeta_{\alpha\gamma}^R \Bigg\{ \overline{n}_1 + \overline{n}_2 - \overline{n}_3 - \overline{n}_4 - \sum_{\beta=1}^{4} \nu_\beta (1 - M_\beta) \times \left[\left(\epsilon_\sigma^* + \frac{1}{2} \right) - \sigma E^* (1 - \delta_{\alpha\beta} - \delta_{\gamma\beta}) \right] \Delta_\beta \Bigg\} \equiv \frac{\tau_\alpha}{x_\alpha^{\rm eq}}, \tag{49}$$

$$\begin{aligned} \frac{{\rm d}\Delta_\alpha}{{\rm d}t} + \frac{{\rm d}\overline{n}_\alpha}{{\rm d}t} &= 2 \sum_{\beta=1}^{4} \zeta_{\alpha\gamma}^E M_\alpha M_\beta (\Delta_\beta - \Delta_\alpha) \\ &+ \frac{1}{3} \zeta_{\alpha\gamma}^R \Bigg\{ \nu_\alpha [2M_\gamma (\epsilon_\sigma^\star + 2) + 3M_\alpha][\overline{n}_1 + \overline{n}_2 - \overline{n}_3 - \overline{n}_4] \\ &+ M_\alpha \sigma \sum_{\beta=1}^{4} \nu_\beta \Bigg[\frac{15}{2} M_\beta - \frac{9}{2} - 3\sigma E^\star (1 - M_\beta)(1 - \delta_{\alpha\beta} - \delta_{\gamma\beta}) \\ &+ 3(\epsilon_\sigma^\star + 2)(1 - M_\beta) \left(1 - \frac{m_\gamma}{m_\alpha} \right) + 4(1 - M_\alpha)(\delta_{\alpha\beta} - \delta_{\gamma\beta})(\epsilon_\sigma^\star + 2) \\ &+ 2\frac{m_\gamma}{m_\alpha} (1 - M_\beta) \left[\epsilon_\sigma^{\star\,2} + 4\epsilon_\sigma^\star + 6 - \sigma (1 - \delta_{\alpha\beta} - \delta_{\gamma\beta}) E^\star (\epsilon_\sigma^\star + 2) \right] \Bigg] \Delta_\beta \Bigg\}, \end{aligned} \tag{50}$$

where α assumes the values 1 to 4 making up a system of eight coupled differential equations for $\overline{n}_\alpha$ and Δ_α.

The system (49) and (50) is solved in subsection 5.2 for three different situations. The first situation corresponds to an initial state with equilibrium concentrations and non-equilibrium temperatures; the second one refers to an initial state with negative affinity and non-equilibrium temperatures for the reactants; the third one is related to an initial state with positive affinity and non-equilibrium temperatures for the products.

5. Analysis of the trend to equilibrium

In order to get explicit results for the reactive system $A_1 + A_2 \rightleftharpoons A_3 + A_4$, the field equations of section 4 will be solved for the elementary reaction $H_2 + Cl \rightleftharpoons HCl + H$. In table 1, the

Table 1. Masses, molecular diameters and formation enthalpy at $T = 298.15$ K.

Gas	H	H_2	Cl	HCl
m_α ($\times 10^{-26}$ kg)	0.167	0.335	5.886	6.054
d_α ($\times 10^{-10}$ m)	1.50	2.90	1.90	3.30
$\Delta_f H_\alpha$ (kJ mol^{-1})	217.97	0	121.68	−92.31

masses m_α and diameters d_α of the gas molecules [9], as well as the corresponding values [37] for the formation enthalpy $\Delta_f H_\alpha$ at $T = 298.15$ K are given. Moreover, for the forward reaction $H_2 + Cl \rightharpoonup HCl + H$, the value [37] of the activation energy ϵ_1 and the value of coefficient A, in the Arrhenius equation $k_1^{(0)} = A\,e^{-\epsilon_1/kT}$, read $\epsilon_1 = 23$ kJ mol^{-1} and $A = 8 \times 10^7$ m^3 mol^{-1} s^{-1}. By considering $T = 298.15$ K, the steric factor for the forward reaction is $s_1 = 0.636$, as it follows from $(39)_1$, and the steric factor for the backward reaction is $s_{-1} = 0.888$, thanks to $(30)_2$. The binding energy difference between products and reactants, E, is related to the enthalpy of the reaction (or reaction heat) by $E = \Delta_r H = \sum_{\alpha=1}^{4} \nu_\alpha \Delta_f H_\alpha$ and for the forward reaction $H_2 + Cl \rightharpoonup HCl + H$, this value reads $\Delta_r H = 3.98$ kJ mol^{-1}. One can assume that the enthalpy of the reaction does not change with the temperature, since the difference between the heat capacities at constant pressure vanishes for gases where the internal degrees of freedom of the molecules—such as rotational and vibrational energies—were not taken into account. Moreover, it will be considered that the mixture's equilibrium particle number density consists of one mole of ideal gas for which $n = 2.6 \times 10^{25}$ molecules m^{-3}. Furthermore, the equilibrium molar fractions $x_\alpha^{\mathrm{eq}} = n_\alpha^{\mathrm{eq}}/n^{\mathrm{eq}}$, with $\sum_{\alpha=1}^{4} x_\alpha^{\mathrm{eq}} = 1$, are restricted by the law of mass action (12). By considering $x_1^{\mathrm{eq}} = x_2^{\mathrm{eq}}$ and $x_3^{\mathrm{eq}} = x_4^{\mathrm{eq}}$, there exists only one molar fraction linearly independent which can be obtained as a function of the temperature from the law of mass action (12), namely

$$\frac{E}{kT} = \frac{3}{2}\ln\left(\frac{m_3 m_4}{m_1 m_2}\right) + 2\ln\frac{2x_1^{\mathrm{eq}}}{\left(1 - 2x_1^{\mathrm{eq}}\right)}. \tag{51}$$

In the numerical simulations which will be performed in the next subsections, two equilibrium temperatures for the mixture, $T_{\mathrm{eq}} = 500$ K and $T_{\mathrm{eq}} = 600$ K, are considered. In subsection 5.1, for $T_{\mathrm{eq}} = 500$ K, the molar fractions are $x_1^{\mathrm{eq}} = x_2^{\mathrm{eq}} = 0.364$ and $x_3^{\mathrm{eq}} = x_4^{\mathrm{eq}} = 0.136$, whereas for $T_{\mathrm{eq}} = 600$ K they are $x_1^{\mathrm{eq}} = x_2^{\mathrm{eq}} = 0.355$ and $x_3^{\mathrm{eq}} = x_4^{\mathrm{eq}} = 0.145$. Conversely, in subsection 5.2, only one value of the equilibrium temperature is considered, $T_{\mathrm{eq}} = 500$ K. In what follows, it should be reminded that subscripts 1, 2, 3 and 4 always stand for H_2, Cl, HCl and H, respectively.

5.1. Asymptotic solutions with constituents at same temperature

The system of linearized differential equations (44) and (46) were solved by imposing the following initial conditions: (i) $\overline{n}_1 = 0.1, \overline{n}_2 = 0.05, \overline{n}_3 = 0.15, \overline{n}_4 = 0.1$ and $\overline{T} = 0$, which means that initially the mixture is at the equilibrium temperature T_{eq} and the affinity is negative, i.e., $\mathcal{A}(0)/kT_{\mathrm{eq}} = -0.1 < 0$ and the direction of the reaction takes place from right to left, and (ii) $\overline{n}_1 = 0.1, \overline{n}_2 = 0.15, \overline{n}_3 = 0.05, \overline{n}_4 = 0.1$ and $\overline{T} = 0$, which also means that the initial temperature of the mixture is the equilibrium one but the affinity is positive, i.e., $\mathcal{A}(0)/kT_{\mathrm{eq}} = 0.1 > 0$ and the reaction takes place from left to right.

In figure 1, it is shown the behaviour of the particle number density perturbations as functions of a dimensionless time $t^\star = t\zeta_R$, where $\zeta_R = 10^8$ Hz is a mean frequency of the reactive collisions. The dashed lines correspond to a mixture with an equilibrium temperature equal to $T_{\mathrm{eq}} = 500$ K, whereas the straight lines refer to $T_{\mathrm{eq}} = 600$ K. The left frame of this

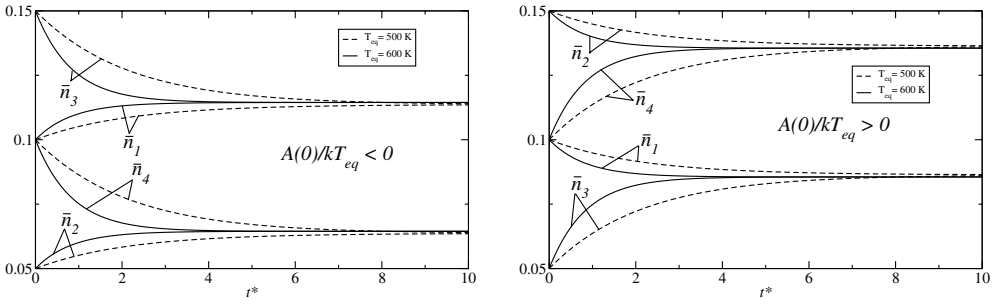

Figure 1. Constituents at the same temperature. Particle number density perturbations versus time for $T_{\rm eq} = 500$ K (dashed lines) and $T_{\rm eq} = 600$ K (solid lines). Left frame: case (i), negative affinity. Right frame: case (ii), positive affinity.

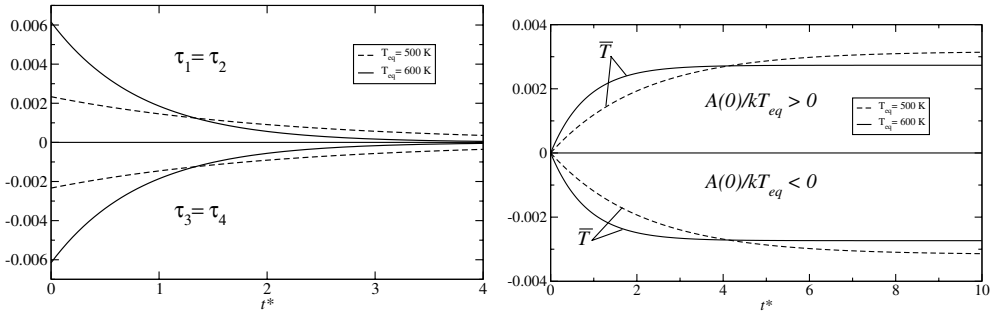

Figure 2. Constituents at the same temperature. Left frame: reaction rate densities versus time for $T_{\rm eq} = 500$ K (dashed lines) and $T_{\rm eq} = 600$ K (solid lines). Right frame: temperature perturbation versus time (case (i) below, case (ii) upper) for $T_{\rm eq} = 500$ K (dashed lines) and $T_{\rm eq} = 600$ K (solid lines).

figure represents case (i) where the affinity is negative and one infers, as was expected, that the perturbations $\overline{n}_1$ and $\overline{n}_2$ for the constituents H_2 and Cl increase, whereas the perturbations $\overline{n}_3$ and $\overline{n}_4$ for the constituents HCl and H decrease. Moreover, the perturbations for H_2 and HCl tend to a same constant value when the time increases, and this behaviour happens also for the constituents Cl and H, indicating that the affinity tends to zero for large values of time and the chemical equilibrium is reached. A similar picture is shown in the right frame of figure 1, case (ii), where the affinity is positive and there exists a decreasing behaviour of the perturbations $\overline{n}_1$ and $\overline{n}_2$ for H_2 and Cl, and an increasing behaviour of $\overline{n}_3$ and $\overline{n}_4$ for HCl and H. In both frames of figure 1, the decay to constant values for the perturbations of the constituents number densities is faster when $T_{\rm eq} = 600$ K.

The time decay of the reaction rate densities is plotted in the left frame of figure 2 for the initial conditions (i) where the affinity is negative. For the case with initial conditions (ii), where the affinity is positive, the behaviour is quite similar provided that $\tau_1 = \tau_2$ is interchanged in the figure by $\tau_3 = \tau_4$. Positive reaction rates, in the upper frame, imply an increasing behaviour of the corresponding number densities $\overline{n}_1$ and $\overline{n}_2$, confirming that the reaction occurs from right to left. As was expected the reaction rate densities become larger by increasing the temperature but decrease more rapidly with time. The right frame of figure 2 represents the behaviour of the temperature perturbation with respect to time, and one infers from this figure that for positive affinities the temperature of the mixture increases and an

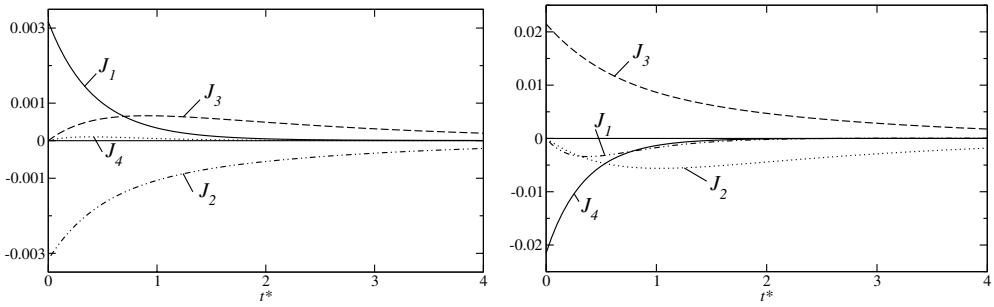

Figure 3. Constituents at the same temperature. Diffusion fluxes versus time for $T_{\rm eq} = 500$ K. Left frame: products initially at rest. Right frame: reactants initially at rest.

exothermic reaction happens, while for negative affinities an endothermic reaction follows, since the temperature of the mixture decreases. Furthermore, the temperature perturbation tends to a constant value more rapidly when the equilibrium temperature of the mixture is higher, since it is connected with the trend to equilibrium of the affinity (see figure 1) or the trend to equilibrium of the reaction rate densities (see figure 2 left).

For the solution of the coupled system of linearized differential equations (45), two sets of initial conditions are imposed. In the first case, $\overline{u}_1 = 0.1, \overline{u}_3 = \overline{u}_4 = 0$, whereas $\overline{u}_2$ is calculated from the constraint $(41)_2$, which represent a diffusion of the constituents H_2 and Cl, the former in the positive x-direction, the latter in the negative one, with the constituents HCl and H at rest. In the second case, $\overline{u}_1 = \overline{u}_2 = 0, \overline{u}_3 = 0.1$, while the value of $\overline{u}_4$ is calculated from the constraint $(41)_2$, which represent a diffusion of the constituents HCl and H, the former in the positive x-direction, the latter in the negative one, with now the constituents H_2 and Cl at rest. The trend to equilibrium of the diffusion fluxes, $J_\alpha = m_\alpha n_\alpha^{\rm eq} \overline{u}_\alpha$, is plotted in figure 3, where now the dimensionless time is given by $t^\star = t\zeta_E$, with $\zeta_E = 4 \times 10^9$ Hz representing a mean collision frequency of the elastic collisions. The left frame refers to the first case. One can infer that the diffusion of the constituents HCl and H happens in the positive x-direction. Moreover, the diffusion flux of the constituent H is very small due to its small mass and the decay of the lighter components H and H_2 occurs more rapidly with time than that of the heavier components Cl and HCl. The right frame of figure 3 represents the time evolution of the diffusion fluxes for the second case, and shows that the diffusion of the constituents H_2 and Cl happens in the negative x-direction. The same conclusion as the former case about the trend to equilibrium of the lighter components H and H_2 can be drawn here, i.e., the decay with time is more pronounced than that of the heavier components Cl and HCl.

5.2. Asymptotic solutions with constituents at different temperatures

The assumption of constituents at different temperatures implies that there exist two 'thermodynamical forces', namely, the one connected with the affinity and the other with the departures from the equilibrium state of the species temperatures, so that the decay of the fields do depend on both thermodynamical forces.

Here three cases are analysed corresponding to different sets of initial conditions, for what deals the partial number density perturbations. Case 1: $\overline{n}_1 = \overline{n}_2 = \overline{n}_3 = \overline{n}_4 = 0$, which means that the initial particle number densities of the constituents are those which define the chemical equilibrium, and therefore the affinity vanishes, i.e. $\mathcal{A}(0)/KT_{\rm eq} = 0$. Case 2: $\overline{n}_1 = 0.1, \overline{n}_2 = 0.05, \overline{n}_3 = 0.15, \overline{n}_4 = 0.1$, which means that the initial affinity is negative, namely $\mathcal{A}(0)/KT_{\rm eq} = -0.1 < 0$. Case 3: $\overline{n}_1 = 0.1, \overline{n}_2 = 0.15, \overline{n}_3 = 0.05, \overline{n}_4 = 0.1$,

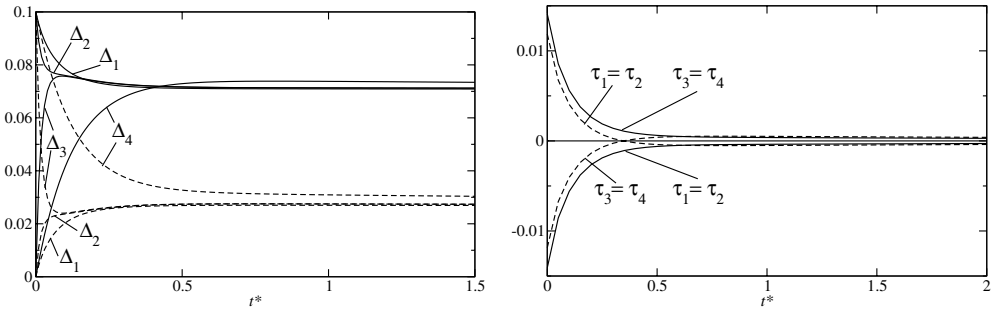

Figure 4. Constituents at different temperature. Case 1: subcase (a) (solid lines); subcase (b) (dashed lines). Left frame: partial temperature perturbations versus time for $T_{\rm eq} = 500$ K. Right frame: reaction rate densities versus time for $T_{\rm eq} = 500$ K.

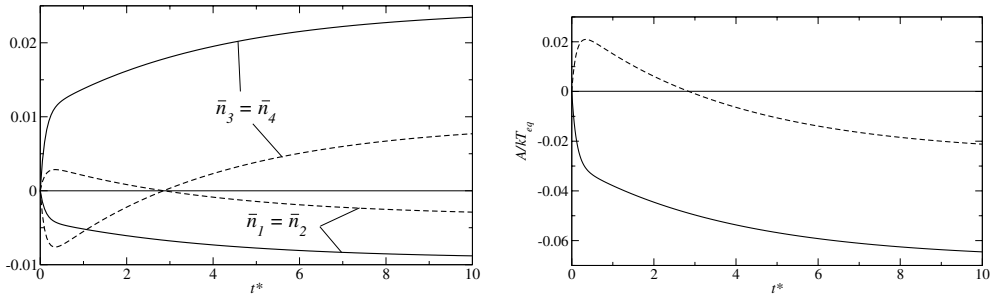

Figure 5. Constituents at different temperature. Case 1: subcase (a) (solid lines); subcase (b) (dashed lines). Left frame: particle number density perturbations versus time for $T_{\rm eq} = 500$ K. Right frame: affinity versus time for $T_{\rm eq} = 500$ K.

which means that the initial affinity is positive, namely $\mathcal{A}(0)/KT_{\rm eq} = 0.1 > 0$. Moreover, for each case, two different situations are considered, namely subcases (a) and (b), with regard to the initial temperatures of the constituents. Subcase (a): $\Delta_1(0) = \Delta_2(0) = 0.1$, $\Delta_3(0) = \Delta_4(0) = 0$, which implies that the initial temperatures of the constituents H_2 and Cl are above the equilibrium temperature. Subcase (b): $\Delta_3(0) = \Delta_4(0) = 0.1$, $\Delta_1(0) = \Delta_2(0) = 0$, which implies that the initial temperatures of the constituents HCl and H are above the equilibrium temperature.

For the first case, the behaviour of the fields are plotted in figures 4 and 5, with the straight lines referring to the initial condition (a) whereas the dashed lines to the initial condition (b). First it is analysed the initial condition (a) where the temperature of constituents H_2 and Cl are above the equilibrium temperature. One can infer from the left frame of figure 4 that the temperature perturbations for the constituents H_2 and Cl decay rapidly with time to a constant value while those for the constituents HCl and H grow rapidly with time and all perturbations tend to the same value for large values of time, i.e., all partial temperatures tend to a common value. In the right frame of figure 4 it is plotted the decay with time of the reaction rate densities. This figure together with the figures for the time evolution of the particle number density perturbations (left frame of figure 5) and of the affinity (right frame of figure 5) show that the particle densities for the constituents H_2 and Cl decay with time whereas those for the constituents HCl and H grow with time and the direction of the reaction takes place from left to right. In case (b) where the constituents HCl and H have temperature above the equilibrium

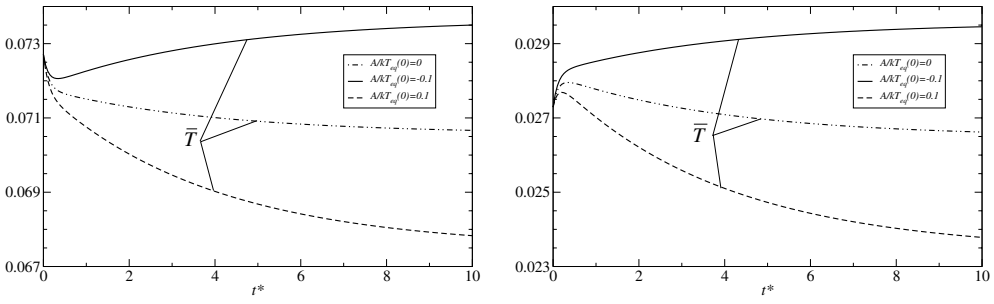

Figure 6. Constituents at different temperature. Perturbations of the mixture temperature versus time for $T_{eq} = 500$ K, for case 1 (dashed-dotted line), case 2 (solid line), case 3 (dashed line). Left frame: subcase (a). Right frame: subcase (b).

one, there exists an abrupt decay of the temperature deviations of these constituents with time which is more pronounced than that of the former case (see figure 4, left frame). Moreover, one can conclude from the time evolution of the reaction rate densities (figure 4, right frame), of the particle number density perturbations (figure 5, left frame) and of the affinity (figure 5, right frame) that during a short period the particle number densities of the constituents HCl and H decay with time but afterwards they grow with time while this behaviour is the opposite for the constituents H_2 and Cl, showing that for a short period of time the direction of reaction takes place from the right to left but afterwards it reverses and takes place from the left to right. Note that the affinity changes its sign during the time evolution.

The perturbations of the mixture temperature are plotted in figure 6 for initial conditions on particle number densities of case 1 (dashed-dotted lines), of case 2 (solid lines) and of case 3 (dotted lines). The left frame refers to initial conditions on temperature differences of subcase (a) whereas the right frame refers to subcase (b). In the case when the constituents H_2 and Cl are initially above the equilibrium temperature of the mixture, the temperature of the mixture decay with time and it happens an endothermic reaction from left to right. However, when the constituents HCl and H have initial temperatures above the equilibrium one, the temperature of the mixture increases implying an exothermic reaction from right to left, followed by a decreasing of this temperature and an endothermic reaction takes place from left to right. One can understand the behaviour of the two cases (a) and (b) described above by invoking Le Châtelier's principle [36] that states: any depart from equilibrium of a thermodynamic variable will induce a trend to equilibrium of the system in order to prevent the imposed modification. In case (a) where the temperatures of the constituents H_2 and Cl are above the equilibrium one, the temperatures of constituents HCl and H must increase to prevent the imposed modification. Moreover, the 'thermodynamical force' related to the affinity tends to compensate that related to the temperature deviations from the equilibrium condition in order to impose a vanishing reaction rate density which characterizes the chemical equilibrium state. Since the temperature deviations never tend to zero, the affinity compensates this behaviour in the opposite direction. For case (b) the temperature of the constituents H_2 and Cl must increase to compensate the imposed modification in the temperatures of the constituents HCl and H. The temperature deviations in this case are smaller than those of the previous case, and the 'thermodynamical force' associated with the affinity compensates rapidly that related to the temperature deviation in such a manner that the rates of change of the perturbations of the particle number densities reverse their signal (see the left frame of figure 5). The reaction proceeds from right to left up to the instant of time where the affinity becomes zero. Since the temperature deviations do not

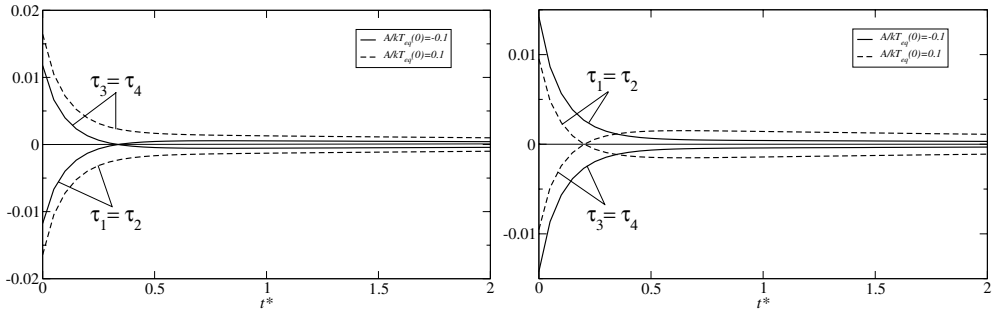

Figure 7. Constituents at different temperature. Reaction rate densities versus time for $T_{\rm eq} = 500$ K, for case 2 (solid line), case 3 (dashed line). Left frame: subcase (a). Right frame: subcase (b).

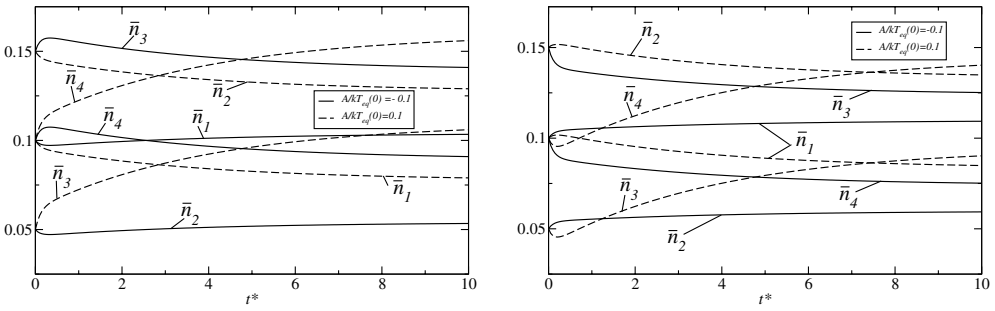

Figure 8. Constituents at different temperature. Particle number density perturbations versus time for $T_{\rm eq} = 500$ K, for case 2 (solid line), case 3 (dashed line). Left frame: subcase (a). Right frame: subcase (b).

vanish at this instant of time the reaction reverses its direction in order to impose a vanishing reaction rate density.

The analysis of the other two cases proceeds as follows. The left frames of figures 7 and 8 represent the time evolution of the reaction rate densities and of the particle number density perturbations, respectively, when the constituents H_2 and Cl are initially at a temperature above the one that characterizes the equilibrium state, (a). The right frame of these figures correspond to the case where the constituents HCl and H have initial temperatures above the equilibrium one, (b). One can infer from the left frames of figures 6, 7 and 8—which refer to the case where H_2 and Cl are above the equilibrium temperature—that for an initial positive affinity an endothermic reaction occurs from left to right. Moreover, for an initial negative affinity the reaction starts from left to right implying an endothermic reaction followed by a reversion in the direction, i.e., from right to left, becoming an exothermic reaction. When the constituents HCl and H are above the equilibrium temperature, one can conclude from the right frames of figures 6, 7 and 8, that for an initial negative affinity an exothermic reaction with the direction from right to left occurs. Furthermore, for an initial positive affinity the direction of the reaction takes place at the beginning from right to left characterizing an exothermic reaction which is followed by an endothermic reaction with a reversion in its direction, namely from left to right. For these two last cases the discussion invoking the Le Châtelier principle proceeds in the same manner as the first case discussed above.

6. Conclusion

In this paper, the extent of the non-equilibrium effects induced by the reversible bimolecular reaction (1), with constituents either at same or different temperatures, has been characterized in a flow regime close to mechanical, chemical and thermal equilibrium, adopting reactive hard spheres cross sections with activation energy. The non-equilibrium effects of the reverse reaction in a quaternary reacting mixture with all constituents at different temperatures have been investigated for the first time in the present paper. Cukrowski *et al* have evaluated these effects in paper [11] assuming deviations of the Mawellian distributions with non-equilibrium concentrations and temperatures, but in the rather simple situation of a symmetric reaction $A + A \rightleftharpoons B + B$ where the constituents have equal masses.

A new strategy founded on a detailed computation of the non-equilibrium production terms and on the solution of the linearized field equations has been adopted, as an alternative to the extended Chapman–Enskog method, widely used in the literature to evaluate the non-equilibrium effects on the velocity distribution functions due to the chemical reaction [2, 9, 24, 28–30, 32], just to cite some pertinent papers.

The detailed computation of the production terms is achieved through a suitably linearized velocity distribution function, which has allowed us to treat, separately, the two cases where the constituents are assumed either at the same or different temperature. In particular, the reactive production terms (36) and (38) for mass and energy of each constituent, due to the reactive mechanism, permit to specify the reaction rate τ_α and temperature T_α of each constituent.

The idea of employing the computation of the production terms, first, leads to a more simplified version of the chemical kinetics analysis of the trend to equilibrium, due to the linearization of the input function performed with respect to the diffusion velocities only. Successively, when the production terms are computed by means of linearized input functions including also the temperature differences of each constituent (see equation (32)), an exhaustive description turns out providing a more detailed analysis of the trend to equilibrium. In the first description, where the constituents have common temperature, the reaction proceeds from right to left for negative values of the affinity and vice versa, making evident the role of the affinity and the trend to equilibrium of the macroscopic fields for the uniform gas (see figures 1–3).

A more complete description of direct and reverse reactions is provided in the second analysis for constituents at different temperatures, since the reaction rate does not depend on the affinity only, but also on other thermodynamic forces related to species temperatures, as shown by (49); see figures 4–8.

Anyway, it appears evident from the numerical simulations of section 5 that a detailed description of the reaction rates, particle number densities and mixture temperature (see figures 1–3), as well as the role of the affinity, is already satisfactory at level of the simplified analysis of subsection 4.1 for which all constituents are assumed at the same temperature. On the other hand, in the more complete analysis of subsection 4.2 for constituents at different temperatures, an exhaustive picture of significant chemical kinetics quantities is obtained, emphasizing the role of species temperatures towards the trend to equilibrium.

In particular, the simulations performed in subsection 5.2 for initial conditions of subcases (a) and (b) regarding the temperatures of constituents with respect to the equilibrium temperature, are also in agreement with Le Châtelier principle, as clearly revealed by figure 6.

It seems reliable that the model here proposed shows a satisfactory performance in the analysis of the asymptotic behaviour of a reacting system for which turbulence effects, as well as Damkohler number effects, do not play any role. On the other hand, from recent

papers dealing with turbulence modelling in the absence of chemical reactions [38–41], one infers that consistent relationships can be stated between kinetic theory and turbulence, even demonstrating that turbulence models can be rigorously derived from Boltzmann kinetic theory [40, 41]. A valid perspective is then to deal with flow regimes including turbulent effects in the frame of extended Boltzmann equation to reacting gases. Such problem however goes beyond the aim of this paper and will be the subject of a future work.

Acknowledgments

The paper is partially supported by Brazilian Research Council (CNPq), by INDAM-GNFM and the National Research Project COFIN 2003 (Coordinator Professor T Ruggeri), and by Minho University Mathematics Centre and Portuguese Foundation for Science and Technology (CMAT-FCT) through the research programme POCTI. One of the authors (GMK) gratefully acknowledges the support and hospitality of the Minho University Mathematics Centre.

References

[1] Kennedy C A 1996 *Bibliography for the Kinetic Theory of Gases* (Livermore: Sandia National Laboratories, Combustion Research Facility)
[2] Shizgal B D and Chikhaoui A 2006 *Physica* A **365** 317
[3] Shizgal B D 1999 *J. Geophys. Res.* **104** 1029
[4] Prigogine I and Xhrouet E 1949 *Physica* **15** 913
[5] Prigogine I and Mahieu M 1950 *Physica* **16** 51
[6] Chapman S and Cowling T G 1970 *The Mathematical Theory of Nonuniform Gases* 3rd edn (Cambridge: Cambridge University Press)
[7] Ross J and Mazur P 1961 *J. Chem. Phys.* **35** 19
[8] Present R D and Morris B M 1969 *J. Chem. Phys.* **50** 151
[9] Shizgal B and Karplus M 1970 *J. Chem. Phys.* **52** 4262
Shizgal B and Karplus M 1971 *J. Chem. Phys.* **54** 4345
Shizgal B and Karplus M 1971 *J. Chem. Phys.* **54** 4357
[10] Cukrowski A S, Popielawski J, Stiller W and Schmidt R 1988 *J. Chem. Phys.* **89** 197
[11] Cukrowski A S, Popielawski J, Qin L and Dahler J S 1992 *J. Chem. Phys.* **97** 9086
[12] Cukrowski A S, Fritzsche S and Popielawski J 1993 *Acta Phys. Pol.* A **84** 369
[13] Eu B C and Li K W 1977 *Physica* A **88** 135
Xystris N and Dahler J S 1978 *J. Chem. Phys.* **68** 374
Xystris N and Dahler J S 1978 *J. Chem. Phys.* **68** 387
[14] Cukrowski A S and Popielawski J 1987 *Acta Phys. Pol.* A **71** 853
[15] Baras F and Malek-Mansour M 1989 *Phys. Rev. Lett.* **63** 2429
[16] Cukrowski A S, Fritzsche S and Popielawski J 1991 *Proc. Int. Symp. of Far-from Equilibrium Dynamics of Chemical Systems* ed J Popielawski and J Gorecki (Singapore: World Scientific)
[17] Malek-Mansour M and Baras F 1992 *Physica* A **188** 253
[18] Nowakowski B and Popielawski J 1994 *Proc. Int. Symp. of Far-from Equilibrium Dynamics of Chemical Systems* ed J Gorecki, A S Cukrowski, A L Kawczynski and B Nowakowski (Singapore: World Scientific) p 293
Cukrowski A S 1994 *Proc. Int. Symp. of Far-from Equilibrium Dynamics of Chemical Systems* ed J Gorecki, A S Cukrowski, A L Kawczynski and B Nowakowski (Singapore: World Scientific) p 309
Cukrowski A S, Gorecki J and Fritzsche S 1994 *Proc. Int. Symp. of Far-from Equilibrium Dynamics of Chemical Systems* ed J Gorecki, A S Cukrowski, A L Kawczynski and B Nowakowski (Singapore: World Scientific) p 329
[19] Nowakowski B and Goreccki J 1996 *Acta Phys. Pol.* B **27** 895
[20] Nowakowski B and Lemarchand A 1997 *J. Chem. Phys.* **106** 3965
[21] Gorecki J, Popielawski J and Cukrowski A S 1991 *Phys. Rev.* A **44** 3791
[22] Gorecki J and Eu B C 1992 *J. Chem. Phys.* **6695** 4345
[23] Alda W, Yuen D A, Luthi H and Rustad J R 2000 *Physica* D **146** 261
[24] Alexeev B V, Chikhaoui A and Grushin I T 1994 *Phys. Rev.* E **49** 2809
[25] Alves G M and Kremer G M 2002 *J. Chem. Phys.* **117** 2205

[26] Kremer G M, Pandolfi Bianchi M and Soares A J 2006 *Phys. Fluids* **18** 037104
[27] Silva A W, Alves G M and Kremer G M 2007 *Physica* A **374** 533
[28] Nowakowski B 1998 *Physica* A **255** 93
[29] Napier D G and Shizgal B D 1995 *Phys. Rev.* E **52** 379
[30] Shizgal B D and Napier D G 1996 *Physica* A **223** 50
[31] Cukrowski A S 2000 *Physica* A **275** 134
[32] Cukrowski A S, Fritzsche S and Fort J 2001 *Chem. Phys. Lett.* **341** 585
[33] Present R D 1955 *Proc. Natl Acad. Sci. USA* **41** 415
[34] Inger G R 2001 *J. Spacecraft Rockets* **38** 185
[35] Prigogine I and Defay R 1973 *Chemical Thermodynamics* (London: Longman)
[36] Kondepudi D and Prigogine I I 1998 *Modern Thermodynamics* (Chichester: Wiley)
[37] Atkins P W 1997 *Physical Chemistry* 5th edn (Oxford: Oxford University Press)
[38] Chen H, Succi S and Orzag S 1999 *Phys. Rev.* E **59** 2527
[39] Succi S, Filippova O, Chen H and Orzag S 2002 *J. Stat. Phys.* **107** 261
[40] Degond P and Lemou M 2002 *J. Math. Fluid Mech.* **4** 257
[41] Ansumali S, Karlin I and Succi S 2004 *Physica* A **338** 379
[42] Chen H, Orzag S, Staroselsky I and Succi S 2004 *J. Fluid Mech.* **519** 301